Available online at www.sciencedirect.com
ScienceDirect
Thin Solid Films 515 (2007) 8424 – 8429
www.elsevier.com/locate/tsf

Direct imaging by atomic force microscopy of surface-localized self-assembled monolayers on a cuprate superconductor and surface X-ray scattering analysis of analogous monolayers on the surface of water

Steen B. Schougaard [a,b,*], Niels Reitzel [c], Thomas Bjørnholm [c], Kristian Kjaer [d,e], Torben R. Jensen [h], Olga E. Shmakova [f], Ramon Colorado Jr. [f], T. Randall Lee [f], J.-H. Choi [g], John T. Markert [g], David Derro [g], Alex de Lozanne [g], John T. McDevitt [b]

[a] *Département de Chimie, Université du Québec à Montréal, Case postale 8888, Succ. Centre-ville, Montréal, Québec, Canada H3C 3P8*
[b] *Texas Materials Institute, Center for Nano and Molecular Science and Engineering, Department Chemistry and Biochemistry, The University of Texas at Austin, Austin, TX, 78722, USA*
[c] *Nano-Science Center, University of Copenhagen, Universitetsparken 5, DK-2100 Copenhagen, Denmark*
[d] *Max-Planck Institute of Colloids and Interfaces, Am Mühlenberg, D-14476 Potsdam/Golm, Germany*
[e] *Niels Bohr Institute, University of Copenhagen, Universitetsparken 5, DK-2100 Copenhagen, Denmark*
[f] *Department of Chemistry, University of Houston, Houston, TX 77204-5003, USA*
[g] *Department of Physics, The University of Texas at Austin, Austin, TX 78712-1081, USA*
[h] *Interdisciplinary Nanoscience Center (iNANO), Department of Chemistry, University of Aarhus, DK-8000 Aarhus C, Denmark*

Received 22 March 2007; accepted 5 April 2007
Available online 18 April 2007

Abstract

A self-assembled monolayer of $CF_3(CF_2)_3(CH_2)_{11}NH_2$ atop the (001) surface of the high-temperature superconductor $YBa_2Cu_3O_{7-x}$ was imaged by atomic force microscopy (AFM). The AFM images provide *direct* 2D-structural evidence for the epitaxial 5.5 Å square $\sqrt{2}\times\sqrt{2}R45°$ unit cell previously predicted for alkyl amines by molecular modeling [J.E. Ritchie, C.A. Wells, J.-P. Zhou, J. Zhao, J.T. McDevitt, C.R. Ankrum, L. Jean, D.R. Kanis, J. Am. Chem. Soc. 120 (1998) 2733]. Additionally, the 3D structure of an analogous Langmuir monolayer of $CF_3(CF_2)_9(CH_2)_{11}NH_2$ on water was studied by grazing-incidence X-ray diffraction and specular X-ray reflectivity. Structural differences and similarities between the water-supported and superconductor-localized monolayers are discussed.

Keywords: Atomic force microscopy; Surface composition; Grazing-incidence X-ray diffraction (GIXD); Self-assembled monolayers (SAMs)

1. Introduction

The process of forming self-assembled monolayers (SAMs) on copper oxide-based high-temperature superconductors is known to remove corrosion products initially and to form densely packed protective layers subsequently [1,2]. SAMs are formed when ceramic or thin-film samples of various copper oxide superconductor materials are exposed to organic or metal organic molecules terminated with an alkylamine group [3–5]. Their structure is of key interest since formation of SAMs offers a convenient way to produce inorganic/organic composite structures with well-defined interfaces. This methodology has been successfully exploited with normal conductors, semiconductors, and insulators [6–8]. Here, we present the first *direct* experimental structural evidence for the formation of highly ordered SAMs of $CF_3(CF_2)_3(CH_2)_{11}NH_2$ atop a (001) surface of the high-temperature superconductor $YBa_2Cu_3O_{7-x}$, as imaged by deflection mode atomic force microscopy (AFM).

The adsorbates employed here differ from those previously studied using computer modeling [1] and reflectance angle infrared spectroscopy [1] since the alkyl chains of the amines are

* Corresponding author. Département de Chimie, Université du Québec à Montréal, Case postale 8888, Succ. Centre-ville, Montréal (Québec), Canada H3C 3P8.
E-mail address: schougaard.steen@uqam.ca (S.B. Schougaard).

0040-6090/$ - see front matter © 2007 Elsevier B.V. All rights reserved.
doi:10.1016/j.tsf.2007.04.034

partially fluorinated to enhance crystallinity and to provide a more robust protective overlayer for the superconductor material [9]. We used two different partially fluorinated adsorbates because preliminary atomic force microscopy (AFM) studies found that only the shorter molecule ($CF_3(CF_2)_3(CH_2)_{11}NH_2$) gave SAMs that showed an ordered registry on the surface of the superconductor; conversely, Langmuir isotherm measurements found that that only the longer molecule ($CF_3(CF_2)_9(CH_2)_{11}NH_2$) gave densely packed Langmuir monolayers on water. Structural characterization of the latter system by both grazing-incidence X-ray diffraction (GIXD) and specular X-ray reflectivity (XR) was needed to establish the structure and order of amine-based partially fluorinated monolayer films, which are reported here for the first time. In particular, we wished to determine whether the structure and packing of the films were influenced by epitaxial registry between the adsorbates and the surface of the superconductor.

2. Experimental details

2.1. Synthesis

The synthesis of the fluorinated amines ($CF_3(CF_2)_n$-$(CH_2)_{11}NH_2$, $n=3$ or 9) has been described previously [10].

2.2. Crystal growth and mounting

The crystal growth and mounting process is similar to the one previously described in Edwards et al. [11]. Briefly, crystals are grown by slow cooling from 1000 °C in a barium copper oxide flux. They are mechanically removed and annealed at 450 °C in flowing oxygen for several weeks and slowly cooled. The resulting thin plate-like crystals (approximately, 1 mm × 1 mm × 20 μm) of $YBa_2Cu_3O_{7-x}$ ($x \approx 0.05$) have the *c* axis perpendicular to the largest surfaces. Crystals were mounted with silver epoxy between two copper wire studs. Excess epoxy was removed using a file before cleaving.

2.3. SAM formation process

$YBa_2Cu_3O_{7-x}$ crystals are cleaved at room temperature in air *immediately* before they are soaked in a 1 mM $CF_3(CF_2)_3$-$(CH_2)_{11}NH_2$/hexane solution (high pressure liquid chromatography grade) for 24 h. The crystals are removed from the solution, thoroughly rinsed with pure hexane, and blown dry with N_2 before transfer to the AFM (Nanoscope III, Digital Instruments). Images were collected in deflection mode, using a standard Si_3N_4 tip (DN-type, Digital Instruments). Care was taken in minimizing the *z*-axis feedback loop gain while mapping the cantilever deflection.

2.4. Grazing-incidence X-ray diffraction (GIXD) and specular X-ray reflectivity (XR)

A monolayer of $CF_3(CF_2)_9(CH_2)_{11}NH_2$ was compressed to a surface area per molecule of $\sim 30 \pm 1$ Å^2 at a surface pressure of $\Pi \sim 35$ mN/m on a pH = 11 subphase at 21.3 ± 0.1 °C. Data were collected using the liquid surface diffractometer [12] at the BW1 undulator beamline [13] at the synchrotron radiation facility HASYLAB, DESY, Hamburg, Germany, using a wavelength of $\lambda = 1.304$ Å monochromated by a Be crystal [14,15]. Two different X-ray techniques were used [12,16,17]: GIXD and XR.

For GIXD, the monolayer was X-ray illuminated at a grazing angle of incidence (α_i) slightly below the critical angle (α_c) for total reflection ($\alpha_i = 0.85\alpha_c$), thus increasing the surface sensitivity by minimizing the penetration depth of the incident X-rays into the water subphase. Any lateral crystallinity in the monolayer will then give rise to Bragg rods [12,16,17]. The scattered X-ray intensity (I) was measured vs. horizontal scattering angle ($2\theta_{xy}$) and vertical exit angle (α_f) and converted to $I(Q_{xy},Q_z)$ where the vertical and horizontal scattering vector components are $Q_z \cong (2\pi/\lambda)\sin(\alpha_f)$ and $Q_{xy} \equiv (Q_x^2 + Q_y^2)^{1/2} \cong (2\pi/\lambda)[1 + \cos^2(\alpha_f) - 2\cos(\alpha_f)\cos(2\theta_{xy})]^{1/2}$ [12,16]. Note that the Langmuir monolayer is a *2D powder*: 2D-crystallites occur that all have their base planes horizontal but represent all azimuthal orientations, so that only $Q_{xy} \equiv (Q_x^2 + Q_y^2)^{1/2}$ can be resolved, not Q_x, Q_y individually.

The XR experiments probe the laterally averaged electron density profile ($\rho(z)$) normal to the interface by varying the incident and exit angles (α_i,α_f) simultaneously ($\alpha_f = \alpha_i \equiv \alpha$), recording the intensity pattern resulting from interference between rays reflected at different depths. Here both laterally crystalline and non-crystalline parts contribute. The measured reflectivity, $R(Q_z)$, normalized to the Fresnel reflectivity, $R_F(Q_z)$, calculated for a theoretical sharp air/water interface, is shown vs. the purely vertical scattering vector $Q_z = (2\pi/\lambda)[\sin(\alpha_i) + \sin(\alpha_f)] = (4\pi/\lambda)\sin(\alpha)$. The XR data were inverted to yield $\rho(z)$ by a method similar to that described in Pedersen and Hamley [18].

3. Results and discussion

One of the significant challenges associated with the direct imaging of cuprate superconductor-localized monolayers has been identifying appropriate sample specimens with surface roughness sufficiently low for these measurements. In the more commonly exploited SAM systems, such as thiols on gold, low roughness can be attained by simply polishing and subsequently annealing the gold surface at elevated temperatures or by evaporating the metal onto cleaved mica [19,20]. Similar protocols cannot be used with the $YBa_2Cu_3O_{7-x}$ system because of its highly reactive nature and complex composition [21]. While previous studies have shown bulk ceramic samples and laser-ablated cuprate films to be suitable for localizing amine monolayers, these samples have proven too rough for structural characterization of the monolayers by AFM.

To overcome these limitations, a procedure for making SAMs using cleaved $YBa_2Cu_3O_{7-x}$ single crystals has been developed. Here, crystals of $YBa_2Cu_3O_{7-x}$ ($x \approx 0.05$) are mounted and cleaved using an adaptation of a previously reported method, whereby the crystals are fragmented at low-temperature for use in STM imaging studies [11]. These studies showed that the cleavage of such crystals occurs primarily

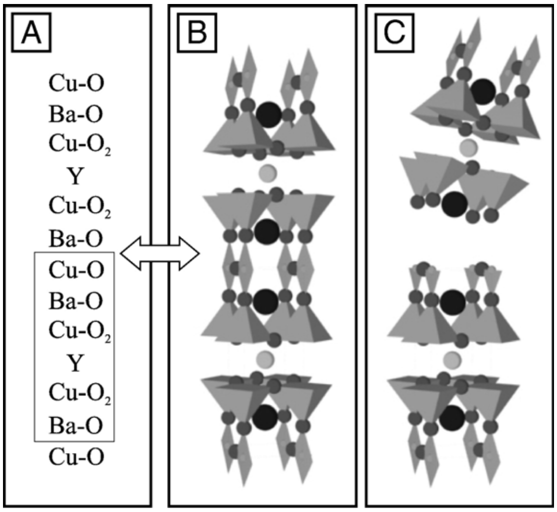

Fig. 1. The crystal structure of $YBa_2Cu_3O_{7-x}$, including the atom labeling scheme (A) for (B) and (C). The box indicates the contents of *one* unit cell. The structure before (B) and after (C) cleavage. The arrow indicates the cleavage plane between the Cu–O chain layer and the Ba–O sheet layer.

between the Cu–O chain layer and the Ba–O sheet layer (Fig. 1) [11].

Initial AFM scans of large areas at low resolution of the SAM atop the cleaved crystal show that the surface roughness is comparable to the highly ordered pyrolytic graphite (HOPG) reference. At higher resolution, atomically resolved AFM images were obtained (Fig. 2A), consistent with a 5.6±0.5 Å square unit cell of area ~31 Å^2. This unit cell does not correlate with any known surface reconstruction of pristine $YBa_2Cu_3O_{7-x}$ [11,22,23], and the 5.6 Å spacing is similar in magnitude to lattice spacings measured for related SAMs on gold derived from partially fluorinated alkanethiols [24]. The unit cell was reproducibly observed in different areas on the crystal surface using various scan areas, different scan directions, and a variety of scan speeds [25]. Examination of the Fourier-transformed image (Fig. 2B) reveals that the peaks are weaker along one reciprocal axis than the other. This phenomenon arises from the striped nature of the direct image, the origin of which is presently unclear. However, it is certain that the stripes are *not* an artifact of the AFM tip, as demonstrated by subsequent scans of the HOPG reference (Fig. 2C).

Highly ordered SAM structures are believed to form primarily due to the interplay between two driving forces [27]: (1) the interaction of the headgroup with the substrate surface, and (2) the lateral intermolecular tail-to-tail interactions. For the specific case of alkylamines adsorbed onto the cuprate superconductor, the two types of interactions are between the amine headgroup and the $YBa_2Cu_3O_{7-x}$ surface, and between the partially fluorinated alkyl chains. Thus, while the square 5.6±0.5 Å repeat unit (of area 31 Å^2) appears to be, within error, consistent with a $\sqrt{2}\times\sqrt{2}R45°$ unit supercell (of area 29.8 Å^2) of the (001) surface [28] (Fig. 3A), it could simply be caused by a maximization of the tailgroup interactions. Therefore, to determine whether the unit cell arises from the registry of the superconductor surface epitaxially, similar

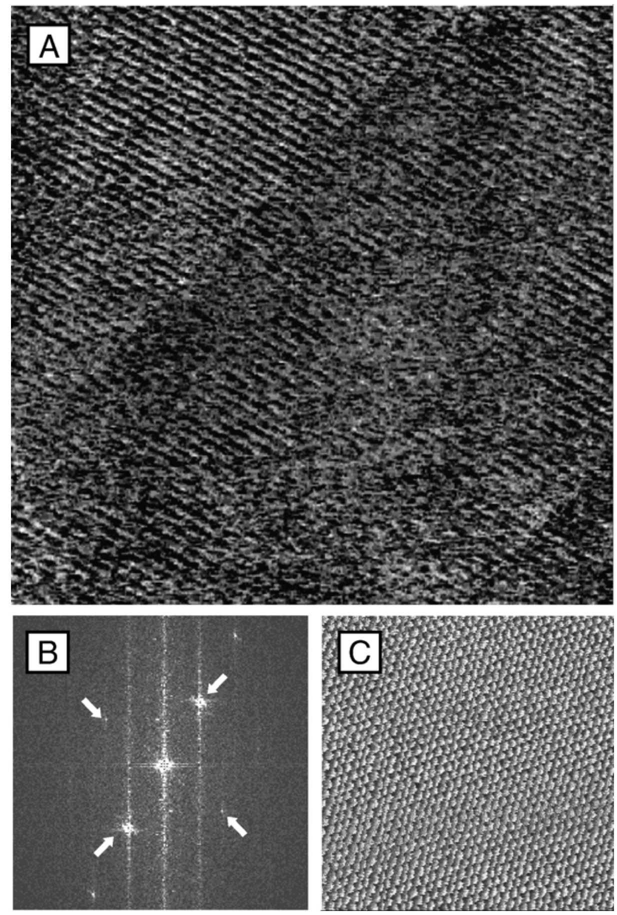

Fig. 2. Direct deflection mode AFM images (30×30 nm) of $CF_3(CF_2)_3(CH_2)_{11}NH_2$ on $YBa_2Cu_3O_{7-x}$ (A). A Fourier-transform of image (A) is shown in (B). Arrows mark the peaks that reflect the square 5.6 Å unit cell. (C) HOPG reference scan (10×10 nm) obtained using the same tip after image A was collected.

monolayers were prepared on water surfaces using the Langmuir method. Having no preferred bonding sites, the surface of liquid water is preferred over solids, such as Au or

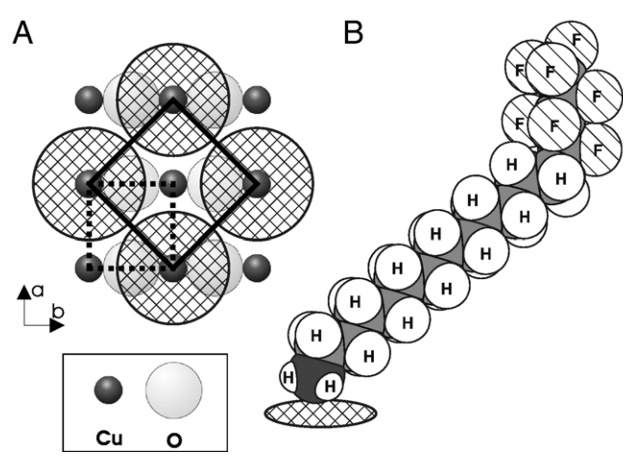

Fig. 3. (A) The proposed superstructure of the amines on the copper oxide chain layer. Dotted line: $YBa_2Cu_3O_{7-x}$ unit cell. Solid line: $\sqrt{2}\times\sqrt{2}R45°$ SAM-superstructure. Note that only every other electrophilic copper site is occupied. (B) Space filling model of the molecule used for the AFM study. The molecular footprint is shown as cross-hatched circles.

Ag. The Langmuir monolayer is therefore primarily defined by the tail-to-tail interactions.

The structural features of the water-localized film compressed to a dense monolayer (Fig. 4) were resolved by means of grazing-incidence X-ray diffraction (GIXD) [12,16,17]. The alkylamine used for this Langmuir film was longer by six CF_2 units than the alkylamine used on $YBa_2Cu_3O_{7-x}$. This substitution was motivated by both experimental and theoretical studies showing that the replacement of flexible hydrocarbons by stiffer fluorocarbons increases the crystallinity of Langmuir films [29,30], which, together with the higher scattering power of fluorine over hydrogen, should enhance the X-ray signal.

GIXD data are shown in Fig. 5 as intensity (grey scale) vs. Q_{xy} and Q_z, the horizontal and vertical components of the scattering vector [12,16]. For a Langmuir film consisting of 2D crystallites all with their base planes horizontal, the Bragg peak at $Q_{xy}=1.255\pm0.02$ Å^{-1} would extend along Q_z as a 'Bragg rod' (at constant Q_{xy}) to ca. $Q_z\leq\pi$/(length of molecule) [16]. In the present data, the observed intensity extends along the *Scherrer ring* of constant $Q^2_{\text{total}}=Q^2_{xy}+Q^2_z$ (full line). This observation is indicative of a mosaic distribution of the orientation of the base planes of the monolayer domains, cf. Fig. 9g,h in ref. [31] and Fig. 2a,b in ref. [32]. Specular X-ray reflectivity data (Fig. 6A) were inverted to yield the laterally averaged electron density distribution $\rho(z)$ across the water/film/air interface (Fig. 6B). Defining $z=0$ (the film/air interface), where ρ is half of its maximum value, a measure of the film thickness, H, may be derived by integrating $\rho(z)A_{\text{mol}}$ from above the interface until, at $z=-H$ (Fig. 6B), the $N=346$ electrons of the molecule are accounted for:

$$N\equiv A_{\text{mol}}\int_{-H}^{+\infty}\rho(z)\mathrm{d}z$$

Using the area per molecule $A_{\text{mol}}=30\pm1$ Å^2 yields $H=26\pm1$ Å. The total length of the molecule should be about 28.7 ± 0.5 Å. However, from space filling considerations (vide infra), we expect the hydrocarbon moiety to be tilted by ca. $48°\pm3°$, giving an expected monolayer thickness of 23.6 ± 0.6 Å, which is similar to the 23 ± 1 Å value measured for a $CF_3(CF_2)_9(CH_2)_{11}SH$ SAM on Au [24]. The larger value of $H=26\pm1$ Å deduced from Fig. 6B might be due to the mosaic distribution inferred from the GIXD data. Indeed, attempts were unsuccessful to fit the reflectivity data (Fig. 6A) with more detailed models of a non-mosaic monolayer. However, semi-quantitatively, the electron density curve (Fig. 6B) seems consistent with the proposed model of a mosaic monolayer with the amine near the water interface and the fluorinated moiety near the air interface.

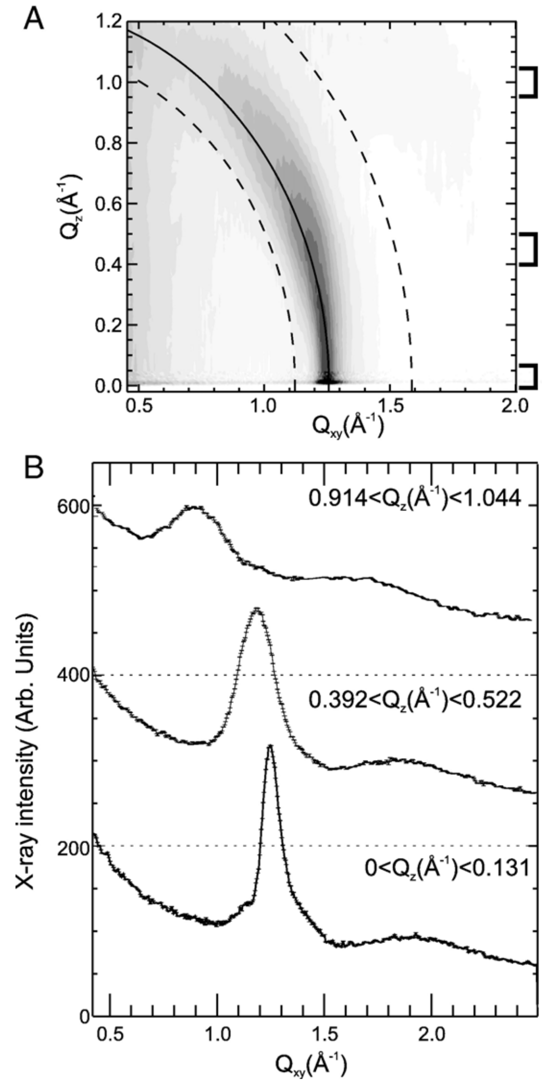

Fig. 5. Grazing-incidence X-ray diffraction data of the $CF_3(CF_2)_9(CH_2)_{11}NH_2$ Langmuir monolayer. (A) Plot of the X-ray intensity (grey scale) vs. Q_{xy} and Q_z, the horizontal and vertical components of the scattering vector [12,16]. (Solid line: The peak of the observed 5.78 ± 0.10 Å hexagonal unit cell. Dashed lines: the hypothetical reflections of a square 5.6 Å unit cell as found in the monolayer on a superconductor surface.) (B) Plotted vs. Q_{xy} is the intensity integrated over the Q_z intervals indicated (and marked with brackets in A). The X-ray wavelength was $\lambda=1.304$ Å.

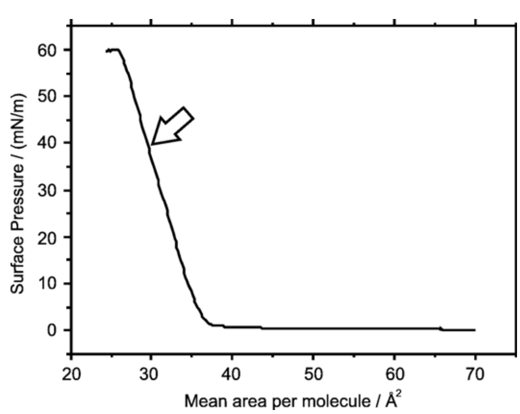

Fig. 4. Compression isotherm of the Langmuir $CF_3(CF_2)_9(CH_2)_{11}NH_2$ monolayer. The arrow indicates the compression at which the X-ray data were gathered.

Comparison between the GIXD measurements of the $CF_3(CF_2)_9(CH_2)_{11}NH_2$ Langmuir film and the predicted peaks of the square unit cell found on the YBCO crystal clearly shows

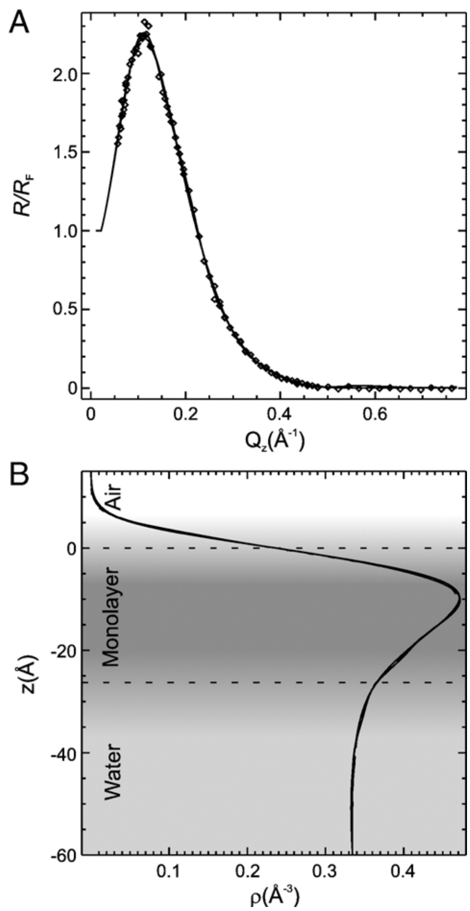

Fig. 6. (A) Specular X-ray reflectivity for the monolayer on water, $R(Q_z)$, normalized by the Fresnel reflectivity, $R_F(Q_z)$, calculated for an ideal abrupt interface between air and bulk water. (B) Electron density profile $\rho(z)$ *on an absolute scale*, inverted from the data in (A). As discussed in the text, $z=0$ is the air–film interface, taken to be where $\rho(z)$ is half is maximum value, and the electron density above $z=-H=-26\pm1$ Å accounts for all of the electrons of the molecule $CF_3(CF_2)_9(CH_2)_{11}NH_2$.

no correlation (Fig. 5A). We thus conclude that the bonding sites of the crystal surface influence the structure of the SAM. Furthermore, when exploring the possible bonding sites for the nucleophilic amine headgroup of *all* possible (001) $YBa_2Cu_3O_{7-x}$ surfaces, the only electrophilic sites that are commensurate with the square 5.6 Å supercell are the copper sites (Fig. 3A) [28]. So, in accordance with previous studies [1,33], it appears that coordination of the amine lone pairs to Cu is responsible for the epitaxy between the SAM and the superconductor.

The three-dimensional SAM structure model is based on a close packed structure that can be accommodated within the AFM unit cell without violating known minimal volume molecular geometry relations. The *area* (29 ± 1 Å^2) of the Langmuir film 2D unit cell ($a=5.78\pm0.10$ Å) (Fig. 5A) combined with the sharp increase in the compression/force curve below ~36 Å^2/molecule (Fig. 4) shows that the 31 ± 3 Å^2 unit cell found on the SAM-covered $YBa_2Cu_3O_{7-x}$ surface can accommodate no more than one molecule. From previous studies of perfluorinated alkanes, it is known that the molecular cross sectional area is ~28 Å^2 [34]. The perfluorinated part of the chain must therefore be approximately perpendicular to the superconductor surface (Fig. 3B). Similarly, previous studies have shown that hydrocarbon chains in close-packed monolayers have a cross-sectional area of ~19–21 Å^2 [35]. Thus, to obtain a close-packed structure, the hydrogenated alkyl chain must be tilted at an angle of approximately arccos(20 Å^2/30 Å^2)$=48°\pm3°$ from vertical as illustrated in Fig. 3B. The kink or bend proposed here between the perfluorinated and hydrocarbon sections is comparable to the ones found in previous structure studies of SAMs derived from partially fluorinated thiols [24,36].

4. Conclusions

We have presented a simple method for generating passivated surfaces of $YBa_2Cu_3O_{7-x}$ sufficiently stable and smooth for atomic scale characterization by AFM. We have then used this technique to provide the first direct evidence for an organized monolayer atop a copper oxide superconductor. The structural motif found is consistent with prior structural models consisting of a $\sqrt{2}\times\sqrt{2}R45°$ superstructure of amines atop the (001) plane of $YBa_2Cu_3O_{7-x}$. The discovery that simple fluorinated amines may form highly ordered and dense monolayers might lead to their use as a molecular blocking layer with sub-nanometer dimensions or as a vehicle for producing more complex organic/inorganic epitaxial structures. This scheme holds promise as it combines the design flexibility inherent to organic/metal organic molecules with the unusual electronic properties of the high-temperature superconductors without compromising the reactive nature of the latter.

Acknowledgments

J. T. McDevitt thanks the AFOSR, NSF (DMR-0211150), TCSUH, and the Welch Foundation for support. S. B. Schougaard thanks the Danish Research Agency for financial support. K. Kjaer thanks the Carlsberg Foundation for financial support. A. de Lozanne thanks the NSF (DMR-0308575) and the Welch Foundation (F-1533) for support. The synchrotron X-ray studies benefited from access to beamline BW1 at HASYLAB at DESY, Hamburg, Germany under the IHP-Contract HPRI-CT-1999-00040/2001-00140 of the European Commission and from support by the Danish Natural Science Research Council's DANSYNC program. T. R. Lee thanks the NSF (DMR-0447588), the Texas Center for Superconductivity, and the Welch Foundation (E-1320) for support. J. T. Markert also thanks the Welch Foundation (F-1191) for support. Dr. D. W. Breiby, Dr. D. A. Vanden Bout, Dr. C. Wells and Dr. J. Mauzeroll are gratefully acknowledged for discussions.

References

[1] J.E. Ritchie, C.A. Wells, J.-P. Zhou, J. Zhao, J.T. McDevitt, C.R. Ankrum, L. Jean, D.R. Kanis, J. Am. Chem. Soc. 120 (1998) 2733.
[2] J.E. Ritchie, W.R. Murray, K. Kershan, V. Diaz, L. Tran, J.T. McDevitt, J. Am. Chem. Soc. 121 (1999) 7447.
[3] F. Xu, K. Chen, R.D. Piner, C.A. Mirkin, J.E. Ritchie, J.T. McDevitt, M.O. Cannon, O. Michael, D.R. Kanis, Langmuir 14 (1998) 6505.

[4] K. Chen, C.A. Mirkin, R.-K. Lo, J. Zhao, J.T. McDevitt, J. Am. Chem. Soc. 117 (1995) 6374.
[5] J.T. McDevitt, S.G. Haupt, C.E. Jones, in: A.J. Bard, I. Rubinstein (Eds.), Electroanalytical Chemistry, vol. 19, Marcel Dekker, New York, 1996, p. 337.
[6] D.L. Allara, Biosens. Bioelectron. 10 (1995) 771.
[7] A. Ulman, An Introduction to Ultrathin Organic Films from Langmuir–Blodgett to Self-Assembly, Academic Press, London, 1991.
[8] A. Ulman, Chem. Rev. 96 (1996) 1533.
[9] H. Fukushima, S. Seki, T. Nishikawa, H. Takiguchi, K. Tamada, K. Abe, R. Colorado Jr., M. Graupe, O.E. Shmakova, T.R. Lee, J. Phys. Chem. 104 (2000) 7417.
[10] T.R. Lee, M. Graupe, U.S. Patent No. 6509100, 21 Jan. 2003.
[11] H.L. Edwards, J.T. Markert, A.L. de Lozanne, J. Vac. Sci. Technol. B 12 (1994) 1886.
[12] T.R. Jensen, K. Kjaer, in: D. Möbius, R. Miller (Eds.), Novel Methods to Study Interfacial Layers, vol. 11, Elsevier, Amsterdam, 2001, p. 205.
[13] R. Frahm, J. Weigelt, G. Meyer, G. Materlik, Rev. Sci. Instrum. 66 (1995) 1677.
[14] J. Als-Nielsen, A.K. Freund, Rev. Sci. Instrum. 63 (1992) 1156.
[15] J. Als-Nielsen, K. Kjaer, Nucl. Instrum. Methods Phys. Res., A 323 (1992) 686.
[16] K. Kjaer, Physica, B 198 (1994) 100.
[17] J. Als-Nielsen, D. Jacquemain, K. Kjaer, F. Leveiller, M. Lahav, L. Leiserowitz, Phys. Rep. 246 (1994) 251.
[18] J.S. Pedersen, I.W. Hamley, J. Appl. Cryst. 27 (1994) 36.
[19] C.A. Alves, M.D. Porter, Langmuir 9 (1993) 3507.
[20] T.M. Schultz, PhD thesis, Aarhus University, 1998.
[21] J.P. Zhou, R.K. Lo, J.T. McDevitt, J. Talvacchio, M.G. Forrester, B.D. Hutn, Q.X. Jia, D. Reagor, J. Mater. Res. 12 (1997) 2958.
[22] H. Behner, K. Rührnschopf, W. Rauch, G. Wedler, Appl. Surf. Sci. 68 (1993) 179.
[23] H.P. Lang, H. Haefke, G. Leemann, H.J. Guntherodt, Physica, C 194 (1992) 81.
[24] K. Tamada, T. Ishida, W. Knoll, H. Fukushima, R. Colorado Jr., M. Graupe, O.E. Shmakova, T.R. Lee, Langmuir 17 (2001) 1913.
[25] AFM images of the unmodified surface could not be obtained presumably due to reaction of the unprotected $YBa_2Cu_3O_{7-x}$ surface with atmospheric water and CO_2 [21,26].
[26] S.B. Schougaard, M.F. Ali, J.T. McDevitt, Appl. Phys. Lett. 84 (2004) 1144.
[27] A.J. Pertsi, M. Grunze, J. Chem. Phys. 106 (1997) 7343.
[28] H. Casalta, P. Schleger, P. Harris, B. Lebech, N.H. Andersen, R. Liang, P. Dosanjh, W.N. Hardy, Physica, C 258 (1996) 321.
[29] M.K. Bernett, M.A. Zisman, J. Phys. Chem. 67 (1963) 1534.
[30] D. Jacquemain, S.G. Wolf, F. Leveiller, F. Frolow, M. Eisenstein, M. Lahav, L. Leiserowitz, J. Am. Chem. Soc. 114 (1992) 9983.
[31] I. Weissbuch, M. Berfeld, W.G. Bouwman, K. Kjaer, J. Als-Nielsen, M. Lahav, L. Leiserowitz, J. Am. Chem. Soc. 119 (1997) 933.
[32] R. Popovitz-Biro, R. Edgar, I. Weissbuch, R. Lavie, S. Cohen, K. Kjaer, J. Als-Nielsen, E. Wassermann, L. Leiserowitz, M. Lahav, Acta Polym. 49 (1998) 626.
[33] J. Zhu, F. Xu, S.J. Schofer, C.A. Mirkin, J. Am. Chem. Soc. 119 (1997) 235.
[34] M.Y. Li, A.A. Acero, Z.Q. Huang, S.A. Rice, Nature 367 (1994) 151.
[35] I. Kuzmenko, V.M. Kaganer, L. Leiserowitz, Langmuir 14 (1998) 3882.
[36] S. Frey, K. Heister, M. Zharnikov, M. Grunze, K. Tamada, R. Colorado Jr., M. Graupe, O.E. Shmakova, T.R. Lee, Isr. J. Chem. 40 (2000) 81.